M 4/2

MODAL REPRESENTATION OF GEOMETRICALLY NONLINEAR BEHAVIOR BY THE FINITE ELEMENT METHOD

D. A. NAGY

Department of Civil Engineering, School of Engineering and Applied Science, Princeton University, Princeton, New Jersey 08540, U.S.A.

SUMMARY

A method is presented for representing mild geometrically nonlinear static behavior of thin-type structures, within the finite element method, in terms of linear elastic and linear (bifurcation) buckling analysis results for structural loading or geometry situations which violate the idealized restrictive (perfect) interpretation of linear behavior up to bifurcation.

Formulation of the finite element displacement method for material linearity but retaining the full, nonlinear strain-displacement relations (geometric nonlinearity) leads to highly nonlinear equations relating the unknown nodal generalized displacements $\underset{\sim}{r}$ to the applied loading $\underset{\sim}{R}$. Restriction to small strains alone does not linearize these equations for thin-type structural configurations; only explicitly requiring that all products of displacement gradients be much smaller than the gradients themselves reduces the equations to the familiar linear form $\underset{\sim}{K}_e\underset{\sim}{r}=\underset{\sim}{R}$, where $\underset{\sim}{K}_e$ is the elastic stiffness. Assuming then that the solution $\underset{\sim}{r}$ of the linear equations also satisfies the full nonlinear equations (i.e., that the above explicit requirement is satisfied), a second solution to the full equations can be sought for a one-parameter loading path $\lambda\underset{\sim}{R}$, leading to the well-known linear (bifurcation) buckling eigenvalue problem $\underset{\sim}{K}_e\underset{\sim}{X}=-\underset{\sim}{K}_g\underset{\sim}{X}\underset{\sim}{\Lambda}$, where $\underset{\sim}{K}_g$ is the geometric stiffness, $\underset{\sim}{X}$ the matrix whose columns are the eigenvectors (so-called buckling mode shapes) and $\underset{\sim}{\Lambda}$ is a diagonal matrix of eigenvalues λ_i (so-called load scale factors).

Approaching the derivations in this manner shows that a sufficient condition for invalidating a linear elastic solution can be expressed in terms of the results of the buckling eigenvalue problem as an examination of the quantities $\underset{\sim}{\alpha}=\underset{\sim}{X}^t\underset{\sim}{R}$ for significant (in terms of the eigenvalue problem solution algorithm) deviation from zero. Further, expansion of the true (nonlinear) solution in terms of basis vectors $\underset{\sim}{X}$ (buckling mode superposition) as $\underset{\sim}{r}(\lambda)=\underset{\sim}{X}\underset{\sim}{\beta}(\lambda)$ shows that, for a class of mildly nonlinear behavior situations, the equations for the coefficients $\underset{\sim}{\beta}$ decouple to yield easily computable expressions $\underset{\sim}{\beta}=[\lambda^{-1}\underset{\sim}{I}-\underset{\sim}{\Lambda}^{-1}]^{-1}\underset{\sim}{\alpha}$ in terms of information contained in a linear elastic and linear buckling finite element analysis. The information also allows the analyst to determine, as a *result* of the analysis, how his particular loading deviates from a perfect bifurcation situation (geometric imperfections can also be considered as equivalent loading imperfections). This is in contrast to most classical analyses in which *a priori* knowledge of the imperfection is required. The severity of the deviation, i.e., whether or not the decoupled equations for $\underset{\sim}{\beta}$ are valid approximations, may also be investigated optionally via the solution of a second buckling eigenvalue problem using the above-mentioned load deviation.

From the viewpoint of the practising structural analyst using finite element software, the method presented here gives broader and deeper significance to an existing linear (bifurcation) buckling analysis capability, in that the additional computations are minimal beyond those already required for a linear static and buckling analysis, and should be easily performable within any well-designed general purpose finite element system. Computational results for braced frame towers and asymmetrically loaded arches (two simple example structures chosen for ease of intuitive insight) illustrate the method and provide good agreement with more expensive full nonlinear finite element analyses.

1. Introduction

A structure of linear elastic material subject to applied forces is strictly in static equilibrium only in its deformed configuration. The resulting force-displacement equations using the exact nonlinear strain-displacement relations, are thus highly nonlinear. The restriction to small strains alone does not alleviate this situation of geometric nonlinearity for "thin" structures (beams, trusses, frames, plates, shells), where large relative rotations may occur without large strain. Only the requirement that all products of displacement gradients be much less than the gradients themselves allows the equations to be fully linearized. Fortunately a very large class of situations of practical interest fulfils this requirement accurately enough; hence the usefulness of linear static analysis. The finite element displacement method applied to these linearized equations has thus yielded a computational method which now forms the backbone of modern structural analysis [1].

The first expansion of the finite element method to treat a very limited type of geometric nonlinear effects led to the formulation of the linear bifurcation buckling eigenvalue problem, the solution of which does not involve a drastic increase in implementational and computational effort beyond that of a linear analysis [2]. Unfortunately, the pure bifurcation phenomenon represented by the linear buckling problem occurs only for certain idealized geometric configurations and loading conditions. Most structural situations modelled in this way actually experience significant nonlinear behavior from the onset of loading, due to geometric imperfections and/or loading irregularities relative to the idealized bifurcation situation. To analyze these situations correctly, recourse was usually made to solution of the full nonlinear behavior equations. The methods developed for such large-displacement analyses [3] all exhibited a large increase in required computational effort in comparison with linear static analysis. This increase in effort plus the recognition that many problem situations are "near bifurcation" has led to suggestions of intermediate analysis methods [4], [5], oriented around representation of the true behavior in terms of the modes and eigenvalues of the linear buckling problem. In particular, certain situations are representable by easily computable linear combinations of these eigenmodes. On the theoretical level, this linear mode superposition method lends much broader significance to the information contained in the solution of the linear buckling analysis software; the major effort in applying the method is still the solution of the linear static and linear buckling problems.

The purpose of this paper is to summarize the essential features of the derivations leading to this method and the computational considerations necessary for its effective practical use. Particular emphasis is placed upon interpretation and justification of the assumptions defining the types of problems for which the method is accurately applicable. Two brief simplified computational examples are presented to illustrate the essential features and accuracy of the method.

2. Theoretical Formulation

2.1 Preliminaries

Let $\underset{\sim}{\varepsilon}$ be a vector of the quantities describing the state of strain at a point in a structure, and $\underset{\sim}{\sigma}$ be the corresponding state of internal stress, in the sense that the product $\underset{\sim}{\sigma}^T\underset{\sim}{\varepsilon}$ (superscript T denotes transpose) is a correct scalar work (energy) value. Similarly let $\underset{\sim}{u}$ be the displacement field and F the corresponding applied force field.

Physical or material linearity implies

$$\sigma = E\varepsilon \tag{1}$$

where E, the material matrix, is not a function of ε. The strain energy of a structure is then

$$U = \frac{1}{2}\int_V \sigma^T \varepsilon dv = \frac{1}{2}\int_V \varepsilon^T E\varepsilon dv \tag{2}$$

where integration is over the material volume. The potential energy of the applied forces, assumed independent of any deformations, is the negative of the work of these forces acting through u,

$$V = -W = \int_V u^T F dv \tag{3}$$

The total potential energy is

$$\pi = U + V \tag{4}$$

The potential energy must be stationary at static equilibrium (principle of virtual displacements or first variation of π)

$$\delta\pi = \int_V (\varepsilon^T E\delta\varepsilon - \delta u^T F)dv = 0 \tag{5}$$

2.2 The Finite Element Displacement Method

The displacement field u is approximated over a discretized structure of finite elements by local interpolation functions, the coefficients of which are related to N nodal generalized displacement values in a vector r. Symbolically

$$u = \phi r \tag{6}$$

where the matrix ϕ contains the element shape functions. With equation (6), the potential energy of applied forces is

$$V = -r^T \int_V \phi^T F dv = -r^T R \tag{7}$$

where

$$R = \int_V \phi^T F dv \tag{8}$$

are the so-called kinematically equivalent nodal applied forces.

The full nonlinear strain-displacement relations can be written, in terms of the finite element approximation (6), as

$$\varepsilon(r) = B^0 r + B^1(r)\cdot r \tag{9}$$

Retention of the second (nonlinear in r) strain component is justified for materially linear behavior in thin-type structures where nonlinear coupling effects are possible without large strain. The matrix B^0 is a function of the shape functions ϕ only, and $B^1(r)$ is a function of ϕ and is linear in r [6]. The strain variation (virtual strain) is then

$$\delta\varepsilon = (B^0 + 2B^1)\delta r \tag{10}$$

Introduction of (6), (8)-(10) into (5) yields for arbitrary δr yields the exact nonlinear equilibrium equations (written in the deformed state)

$$\int_V (\underset{\sim}{B}^0 + 2\underset{\sim}{B}^1)^T \underset{\sim}{\sigma} dv = \underset{\sim}{R} \tag{11}$$

where, from (1)

$$\underset{\sim}{\sigma} = \underset{\sim}{E}(\underset{\sim}{B}^0 + \underset{\sim}{B}^1)\underset{\sim}{r} \tag{12}$$

Neither assumption of small strains $\underset{\sim}{\varepsilon}$ nor small displacements $\underset{\sim}{r}$ is sufficient to linearize (11) for certain thin structural configurations of interest. Substitution of (12) into (11) gives explicit nonlinear equations between total $\underset{\sim}{R}$ and total $\underset{\sim}{r}$ as

$$[\underset{\sim}{K}_e + \underset{\sim}{K}_g(\underset{\sim}{\sigma}) + \underset{\sim}{K}_l(\underset{\sim}{r})]\underset{\sim}{r} = \underset{\sim}{K}_s\underset{\sim}{r} = \underset{\sim}{R} \tag{13}$$

where

$$\underset{\sim}{K}_e = \int_V \underset{\sim}{B}^{0T}\underset{\sim}{E}\underset{\sim}{B}^0 dv \tag{14}$$

$$\underset{\sim}{K}_g = 2\int_V \underset{\sim}{C}(\underset{\sim}{\sigma}) dv \tag{15}$$

$$\underset{\sim}{K}_l = \int_V \underset{\sim}{B}^{0T}\underset{\sim}{E}\underset{\sim}{B}^1(\underset{\sim}{r}) dv \tag{16}$$

The notation $\underset{\sim}{K}_s$ is used to emphasize that the relation between $\underset{\sim}{r}$ and $\underset{\sim}{R}$ is a secant (total) stiffness. The matrix $\underset{\sim}{C}$ in (15) is symmetric, linear in the stress vector $\underset{\sim}{\sigma}$, and closely related in form to $\underset{\sim}{B}^1$ (see [6]). Formal differentiation of (13) with respect to $\underset{\sim}{r}$ leads to the tangent stiffness formulation which forms the basis for most currently used incremental/iterative nonlinear analysis algorithms.

2.3 Linearization of the Governing Equations

If all products of displacement gradients are ignorable with respect to the displacement gradients themselves, then the strain-displacement relations can be linearized. For a one-parameter family of displacement states $\lambda\underset{\sim}{r}$, this situation is denoted symbolically as

$$|\lambda\underset{\sim}{B}^1\cdot\underset{\sim}{r}| << |\underset{\sim}{B}^0\underset{\sim}{r}| \tag{17}$$

which implies that magnitudes of all nonzero scalar quantities on the left-hand side are ignorable with respect to corresponding quantities on the right-hand side. The precise meaning of "ignorable" is of course a subjective choice of the structural analyst, and the accuracy of analysis results must be viewed in the same subjective context. This point is unfortunately often forgotten in practice.

Use of (17) directly in (9) leads to $\delta\underset{\sim}{\varepsilon} = \underset{\sim}{B}^0\delta\underset{\sim}{r}$ and $\underset{\sim}{\sigma} = \underset{\sim}{E}\underset{\sim}{B}^0\underset{\sim}{r}$, so that the equations (13) reduce to the standard form

$$\underset{\sim}{K}_e\underset{\sim}{r} = \underset{\sim}{R} \tag{18}$$

of linear static analysis, where $\underset{\sim}{K}_e$ is the elastic stiffness matrix. The assumptions (17) could also be introduced at later stages in the derivations leading to (13). In particular, using (17) only in (13) itself yields

$$[\underset{\sim}{K}_e + \underset{\sim}{K}_g(\underset{\sim}{\sigma}_L)]\underset{\sim}{r} = \underset{\sim}{R} \tag{19}$$

where $\sigma_L = \underset{\sim}{E}\underset{\sim}{B}^0\underset{\sim}{r}$ (linear stresses) (20)

The form (19) is equivalent to (18) only if

$$|\underset{\sim}{K}_g(\underset{\sim}{\sigma}_L)\cdot\underset{\sim}{r}| << |\underset{\sim}{K}_e\underset{\sim}{r}| \qquad (21)$$

which, as shown below, provides a useful practical test for the validity (accuracy) of a linear static solution.

2.4 Alternate Equilibrium States: Bifurcation

A displacement solution $\lambda\underset{\sim}{r}_1$ of (18) for a one parameter loading family $\lambda\underset{\sim}{R}_1$ is termed a true linear solution if it satisfies (i.e., the equation error is ignorable in the sense of (17)) the full nonlinear equations (13). Since equations (13) are nonlinear, however, it is reasonable to assume that they have solutions other than $\lambda\underset{\sim}{r}_1$. Taking these in the form of perturbations to $\lambda\underset{\sim}{r}_1$,

$$\underset{\sim}{\hat{r}} = \lambda\underset{\sim}{r}_1 + \Delta\underset{\sim}{r} \qquad (22)$$

introducing (22) into (13), and ignoring higher-order terms in $\Delta\underset{\sim}{r}$, leads to the well-known linear buckling eigenvalue problem

$$\underset{\sim}{K}_e\underset{\sim}{X} = -\underset{\sim}{K}_g(\underset{\sim}{\sigma}_{1L})\underset{\sim}{X}\underset{\sim}{\Lambda} \qquad (23)$$

where $\underset{\sim}{\sigma}_{1L}$ are the linear stresses due to loading $\lambda\underset{\sim}{R}_1$; $\underset{\sim}{\Lambda}$ is a diagonal matrix of λ-values, arranged in order of non-decreasing magnitude, representing the load scale factors in (22), and $\underset{\sim}{X}$ contains the corresponding shapes of $\Delta\underset{\sim}{r}$ as its columns. The classical interpretation of (23), namely that the structure buckles at $\lambda = \lambda_1$ (first diagonal element in $\underset{\sim}{\Lambda}$), is based on the assumption that $\lambda\underset{\sim}{r}_1$ satisfies (13) up to $\lambda = \lambda_1$, which implies that it also satisfies (21). Unfortunately, most practical analysis situations do not fulfill these idealized limiting states for thin-type structures due to loading and/or geometry imperfections. Thus (21) appears, at first, to be an indicator of whether linear static and linear buckling results are valid according to the classical interpretation. In cases where they are not valid, they may still be used to approximate the actual nonlinear behavior, as is shown below.

It is convenient to transform (23) to the standard form

$$\underline{A}\underline{Y} = \underline{Y}\underline{\Omega} \qquad (24)$$

using

$$\underline{A} = \underline{U}^{-T}\underline{K}_g\underline{U}^{-1} \qquad (25)$$

$$\underline{Y} = \underline{U}\underline{X} \qquad (26)$$

$$\underset{\sim}{\Omega} = -\underset{\sim}{\Lambda}^{-1} \qquad (27)$$

$$\underline{U}^T\underline{U} = \underset{\sim}{K}_e \qquad (28)$$

where $\underline{U}$ is the upper triangular Cholesky factor of $\underline{K}_e$. With $\underline{Y}$ taken to be an orthogonal matrix ($\underline{Y}^T\underline{Y} = \underline{Y}\underline{Y}^T = \underline{I}$),

$$\underline{X}^T\underline{K}_e\underline{X} = \underline{I} \qquad (29)$$

$$\underline{X}^T\underline{K}_g\underline{X} = -\underline{\Lambda}^{-1} \qquad (30)$$

2.5 A Class of Mild Nonlinear Solutions

A class of loadings $\lambda \underset{\sim}{R}$, which produce linear solutions $\lambda \underset{\sim}{r}_L$ from (18) that do not satisfy (17), is assumed to be "close" to some loading $\lambda \underset{\sim}{R}_1$ whose linear elastic solution $\lambda \underset{\sim}{r}_1$ does satisfy (17). The meaning of "close" is clarified below. Let

$$\lambda \underset{\sim}{R} = \lambda (\underset{\sim}{R}_1 + \Delta \underset{\sim}{R}) \tag{31}$$

The true (nonlinear) solution of (13) for loading $\lambda \underset{\sim}{R}$ can also be represented as

$$\underset{\sim}{r}(\lambda) = \lambda \underset{\sim}{r}_1 + \Delta \underset{\sim}{r} \tag{32}$$

where, due to the nonlinearities, $\Delta \underset{\sim}{r}$ is not just the displacement due to $\lambda \Delta \underset{\sim}{R}$ in (31). But the fact that $\lambda \underset{\sim}{r}_1$ is a true linear solution for $\lambda \underset{\sim}{R}_1$, and the assumption that $\|\Delta \underset{\sim}{r}\| << \|\lambda \underset{\sim}{r}_1\|$ ($\|a\|$ denotes a norm of a vector $\underset{\sim}{a}$) leads to representation of (13) as

$$\lambda \underset{\sim}{K}_e \underset{\sim}{r}_1 + \underset{\sim}{K}_e \Delta \underset{\sim}{r} + \underline{\lambda \underset{\sim}{K}_g (\underset{\sim}{\sigma}_{1L}) \Delta \underset{\sim}{r}} = \lambda \underset{\sim}{R}_1 + \lambda \Delta \underset{\sim}{R} \tag{33}$$

by ignoring higher-order terms in $\Delta \underset{\sim}{r}$. The underlined term in (33) represents a non-ignorable nonlinear coupling term between the dominant linear stress system $\underset{\sim}{\sigma}_{1L}$ and geometry change $\underline{\Delta r}$, as would be expected intuitively from simple classical buckling situations. Unfortunately, (33) is not solvable since neither $\lambda \underset{\sim}{R}_1$ nor $\lambda \underset{\sim}{r}_1$ is known. Since only $\lambda \underset{\sim}{R}$ (the actual applied loading) is known, what is actually sought is a solution method for $\underset{\sim}{r}_d(\lambda)$ where

$$\underset{\sim}{r}(\lambda) = \lambda \underset{\sim}{r}_L + \underset{\sim}{r}_d(\lambda) \tag{34}$$

Substitution of (34) into (33), using (32) and some manipulation, produces

$$\underset{\sim}{K}_e \underset{\sim}{r}_d + \lambda \underset{\sim}{K}_g (\underset{\sim}{\sigma}_{1L}) \underset{\sim}{r}_L + \lambda \underset{\sim}{K}_g (\underset{\sim}{\sigma}_1) \underset{\sim}{r}_d = 0 \tag{35}$$

Note that (35) still contains the unknown stress state $\underset{\sim}{\sigma}_{1L}$ corresponding to $\underset{\sim}{r}_1$.

2.6 Change of Basis Vectors: Mode Superposition

Since the columns of (NxN) matrix $\underset{\sim}{X}$ span an N-dimensional vector space, they are now introduced as new basis vectors for the various displacement vectors. In particular,

$$\underset{\sim}{r}_L = \underset{\sim}{X} \underset{\sim}{\alpha} \tag{36}$$

$$\underset{\sim}{r}_d = \underset{\sim}{X} \underset{\sim}{\gamma}(\lambda) \tag{37}$$

$$\underset{\sim}{r}(\lambda) = \underset{\sim}{X} \underset{\sim}{\beta}(\lambda) = \underset{\sim}{X}(\lambda \underset{\sim}{\alpha} + \underset{\sim}{\gamma}) \tag{38}$$

This procedure, in essence, represents the sought (unknown) true nonlinear displacements as a linear combination of the modes of problem (23). The coefficients of combination $\underset{\sim}{\beta}$ are often termed the generalized coordinates of the transformed problem. Introducing (36)-(38) into (35), premultiplying by $\underset{\sim}{X}^T$, and using (29), yields

$$\underset{\sim}{\gamma} + [\underset{\sim}{X}^T \underset{\sim}{K}_g (\underset{\sim}{\sigma}_{1L}) \underset{\sim}{X}](\lambda^2 \underset{\sim}{\alpha} + \lambda \underset{\sim}{\gamma}) = \underset{\sim}{0} \tag{39}$$

The term in brackets is, however, diagonalized (30) only by the unknown modes $\underset{\sim}{X}$ corresponding to the unknown stress state $\underset{\sim}{\sigma}_{1L}$. Here, it is now possible to precisely specify the original assumption of "closeness" made in Section 2.5 above:

> The distortion of the eigenvalue problem (23) by the addition of stresses $\underset{\sim}{\sigma}_2 = \underset{\sim}{E}\underset{\sim}{B}^0 \underset{\sim}{K}_e^{-1} \Delta \underset{\sim}{R}$ is negligible, i.e., the differences between the eigenvalues and eigenvectors found using $\underset{\sim}{\sigma}_{1L} = \underset{\sim}{E}\underset{\sim}{B}^0 \underset{\sim}{K}_e^{-1} \underset{\sim}{R}_1$ and $\underset{\sim}{\sigma}_L = \underset{\sim}{E}\underset{\sim}{B}^0 \underset{\sim}{K}_e^{-1} \underset{\sim}{R}$ can be ignored.

The mathematical and physical meaning of this assumption is examined in [7]. Its use decouples (39) to give

$$\underset{\sim}{\gamma} = \lambda^2[\underset{\sim}{\Lambda} - \lambda\underset{\sim}{I}]^{-1}\underset{\sim}{\alpha} \tag{40}$$

and thus

$$\underset{\sim}{r}(\lambda) = \underset{\sim}{X}\left[\frac{1}{\lambda}\underset{\sim}{I} - \underset{\sim}{\Lambda}^{-1}\right]^{-1}\underset{\sim}{\alpha} \tag{41}$$

where $\underset{\sim}{\Lambda}$ and $\underset{\sim}{X}$ are obtained from (23) for the known stresses $\underset{\sim}{\sigma}_L$. The $\underset{\sim}{\alpha}$ values are computed from

$$\underset{\sim}{X}^T\underset{\sim}{R} = \underset{\sim}{X}^T\underset{\sim}{K}_e\underset{\sim}{r}_L = \underset{\sim}{X}^T\underset{\sim}{K}_e\underset{\sim}{X}\underset{\sim}{\alpha} = \underset{\sim}{\alpha} \tag{42}$$

2.7 Properties and Physical Interpretations

The N conditions (21), which are a test of true linearity of any solution of (18), i.e., are necessary conditions for linearity, may be transformed, via premultiplication by $\underset{\sim}{X}^T$ and using (36), to

$$|\lambda\underset{\sim}{\Lambda}^{-1}\underset{\sim}{\alpha}| << |\underset{\sim}{\alpha}| \tag{43}$$

In terms of the eigenvalue spectrum in $\underset{\sim}{\Lambda}$, (43) implies the following: if j+1 is the first eigenvalue in $\underset{\sim}{\Lambda}$ for which

$$\left|\frac{\lambda_1}{\lambda_j}\right| << 1 \ , \quad 1 < (j+1) < N \tag{44}$$

then a solution $\lambda\underset{\sim}{r}_L$, $\lambda < \lambda_1$, is linear only if the elements α_i of $\underset{\sim}{\alpha}$ satisfy

$$\alpha_i \equiv 0 \qquad i=1,2,\ldots,j \tag{45}$$

For most practical problems j << N, which is what makes this method computationally attractive. For solutions $\lambda\underset{\sim}{r}_L$ not satisfying (45), it is possible now to find the load deviation $\Delta\underset{\sim}{R}$ of (31) as

$$\Delta\underset{\sim}{R} = \sum_{i=1}^{j} \alpha_i\underset{\sim}{K}_e\underset{\sim}{X}_i \tag{46}$$

where $\underset{\sim}{X}_i$ is the i^{th} column of $\underset{\sim}{X}$. Then the so-called "perfect" loading which would cause true linear bifurcation buckling is just

$$\underset{\sim}{R}_1 = \underset{\sim}{R} - \Delta\underset{\sim}{R} \tag{47}$$

From (44) and (40), it is seen that only the first j modes contribute to the nonlinearity in (41), so that the eigenvalue problem (23) need only be solved for the first j vectors in $\underset{\sim}{X}$. For large problems, a considerable savings in computational effort could be expected over a full iterative nonlinear analysis if j << N.

The assumption $||\Delta\underset{\sim}{r}|| << ||\lambda\underset{\sim}{r}_1||$ used in obtaining (33) can also be expressed, via energy norms, in terms of known quantities to provide a measure of whether (41) is sufficiently accurate [7].

2.8 Geometric Imperfections

The classical concept defines geometry imperfections as slight geometric deviations of a given structure from a perfect (symmetric) bifurcation-type situation [8]. But in an actual finite element analysis, only the given geometry is known.

Such cases can be transformed by the assumption that the given structure, whatever its actual geometry, has <u>some</u> nonzero loading which produces ideal linear bifurcation buckling behavior. This assumption implies that $j < N$, i.e., that a nonzero $\underset{\sim}{R}_1$ exists in (47). The loading deviation $\Delta\underset{\sim}{R}$ is thus a <u>loading imperfection</u>. This approach is advantageous for an automated, production-oriented finite element analysis since it is not usually desirable (or often even possible) to have to recognize and specify some neighboring "perfect" geometry as additional input data. All that is required here is the known geometry and known applied loading.

3. Computational Considerations

3.1 Implementation

Actual implementation of the mode superposition method in any large, modern finite element software system which performs a linear buckling analysis involves no additional programming since the capabilities required should already be present in such software. This is made clearer by summarizing the basic steps of the method:

1. Linear elastic solution (18) for given loading $\underset{\sim}{R}$.
2. Linear buckling analysis (23) using stresses found in Step 1, for $j \ll N$ eigenpairs λ_i, $\underset{\sim}{x}_i$.
3. Computation of $\underset{\sim}{\alpha}$-values from (42) (simple matrix multiplication).
4. Test for true linearity of solution $\underset{\sim}{r}_L$ from step 1 via (45).
5. If test not satisfied, test whether energy in first j modes is much smaller than total linear energy [7]

$$\sum_j \alpha_i^2 \ll \underset{\sim}{R}^T \underset{\sim}{r}_L \tag{48}$$

6. If (48) is satisfied, compute $\underset{\sim}{r}(\lambda)$ using (41).

An addition test which is more time consuming, involving the load deviation $\Delta\underset{\sim}{R}$ (46), could also be performed when desirable using standard buckling analysis software and the loading $\underset{\sim}{R}_1$ (47). See [7] for more discussion.

3.2 Significance of α-values

The test in step 4 above tests values of $\underset{\sim}{\alpha}$ against zero according to (45). Although they should be zero <u>theoretically</u> for a true linear solution $\underset{\sim}{r}_L$, the <u>computed</u> values of $\underset{\sim}{\alpha}$ from (42) contain numerical error related to error in the buckling mode shapes $\underset{\sim}{X}$. The transformed eigenproblem (24) is usually solved iteratively (e.g., by simultaneous vector iteration [9]) so that the resulting eigenvectors $\underset{\sim}{Y}$ (and hence $\underset{\sim}{X}$ via (26)) contain small residual errors. Thus it is necessary, for actual computer implementation and use, to develop a test of whether the computed $\underset{\sim}{\alpha}$-values are significantly nonzero, i.e., whether their deviation from zero is due to nonlinear behavior and not just to residual error in $\underset{\sim}{X}$.

A detailed examination of the residuals in $\underset{\sim}{X}$ (space limitations prevent its presentation here), plus certain assumptions involving norms and subspaces of eigenvectors, leads to computable bounds on the amount of numerical error which could be contained in α when the theoretical values $\underset{\sim}{\alpha}_i$ are zero [7]. Specifically, if

$$\frac{(\alpha_i)_c}{(\underset{\sim}{\alpha}^T\underset{\sim}{\alpha})^{\frac{1}{2}}} \gg \frac{(\underset{\sim}{\eta}_i^T\underset{\sim}{\eta}_i)^{\frac{1}{2}}|\lambda_i\lambda_m|}{|\lambda_i - \lambda_m|} \qquad i=1,2,\ldots,j \tag{49}$$

then the information content (related to nonlinearity) in $\underset{\sim}{\alpha}$ is significant, i.e., the test in step 4 above can be judged to not be satisfied. In (49), $\underset{\sim}{\eta}_i$ is the residual in the i^{th} eigenvector (i^{th} column of $\underset{\sim}{Y}$) and λ_m is the closest eigenvalue outside the subspace which was iterated (i.e., $m > j$; if all λ_i are positive, $m = j+1$).

4. Numerical Examples

4.1 Remarks on Software Used

The numerical examples used so far to test, study, and confirm the linear mode superposition method have been calculated entirely within the ASKA finite element system [10], [11]. This is thus an illustration of the comments made above concerning implementation, since no modifications or extensions of ASKA were necessary, although it had not been originally developed with the mode superposition method in mind. For comparison purposes, full iterative Newton-Raphson nonlinear analyses were performed on the various problems [6]. Since these full nonlinear analyses were not performed using ASKA, a comparison of execution times would not be very meaningful. This is particularly true since the small, simple examples chosen here to best illustrate the method are not the production-size problems for which a system like ASKA is intended to be most effective.

4.2 Braced Truss Tower

The tower shown in Figure 1 is chosen as a simple structure which is expected to behave qualitatively like the classical pin-ended Euler column in buckling. Loading case a) is expected to be an idealized case of pure bifurcation buckling. The computed $\underset{\sim}{\alpha}$-values bear out this expectation: none of them satisfy the significance test (49). Case b), with the slight load "deviation" represented by the lateral load at midheight, on the other hand, produces a significantly nozero value of α_1 and a nonlinear behavior $\underset{\sim}{r}(\lambda)$; the component of $\underset{\sim}{r}(\lambda)$ representing lateral motion at midheight (on the opposite side from the lateral load) is plotted in Figure 2, where good agreement with the full nonlinear analysis is evident. The lateral load imperfection, in essence, activates the first buckling mode, i.e., the lateral displacements caused by this part of the loading couple with the dominant "axial" (vertical) force system to amplify the lateral displacements nonlinearly. Other loading case results, which cannot be shown here due to space restrictions, show the method's ability to represent off-center vertical loading, more complicate lateral loading patterns, load reversal, and geometry imperfections adequately [7]. Results presented in [7] also show that the eigenvalue problem (23) is not significantly distorted by the presence of a side load as in case b), even when the magnitude of that load is of the same order as the vertical loads, a result which verifies the definition of closeness given in Section 2.6 above.

4.3 Symmetric Arches under Asymmetric Loading

The symmetric circular arch segment with built-in ends is subject to an asymmetric vertical loading as shown in Figure 3. It has been shown (e.g., [12]) that the parameter $K = R\theta^2/h$ governs whether symmetric (snap-through) or antisymmetric (bifurcation) buckling occurs first for symmetric loadings. For values $K > 5.024$ bifurcation occurs first. The results of applying the mode superposition method to the asymmetric loading of Figure 3, for $K = 40$, are plotted in Figure 4 for the radial displacement of point P (quarter-point), and good agreement is again seen with the full nonlinear results. It is interesting to note that the test (48) was not satisfied in this case, i.e., the mode superposition method should not necessarily be as accurate as Figure 4 indicates. This is probably evidence that the test (48) is too conservative. Other examples involving arches and axially-loaded cylindrical shell segments are presented in [2], [7].

5. Conclusions and Further Research

The linear mode superposition method outlined here shows promise of providing accurate results, based on a linear buckling analysis, for mild nonlinearities not previously thought to be analyzable in such terms. From a practical viewpoint, it gives broader significance and utility to existing linear buckling analysis capabilities in finite element analysis.

The examination of the higher-order terms in $\Delta \underset{\sim}{r}$, ignored in arriving at (33), and consideration of appropriate solution algorithms using these terms, is the subject of current ongoing research. In particular, inclusion of such terms should facilitate analysis into the so-called post-buckling range of loading and contain the information characterizing what is usually termed imperfection sensitivity.

The basis change introduced in Section 2.6 should achieve a type of condensation in that the equations for $\underset{\sim}{\beta}$, although no longer decoupled as in the linear mode superposition method, are nevertheless a much smaller system of nonlinear algebraic equations than e.g., the system (13). An important aspect of the current work is to examine the efficiency and automatability of such intermediate nonlinear analysis methods involving condensation, in comparison with general nonlinear methods, for a wider range of practical problems.

6. References

[1] ARGYRIS, J.H., "Continua and Discontinua," Opening Paper to the Air Force Conference on Matrix Methods in Structural Mechanics, Dayton, Ohio, U.S.A., October 1965.

[2] KÖNIG, M., NAGY, D.A., and STREINER, P., "Linear Buckling Analysis with the ASKA Program System," Int. J. of Computer Methods in Applied Mechanics and Engineering (to appear).

[3] ODEN, J.T., Finite Elements of Nonlinear Continua, McGraw-Hill, New York, 1972.

[4] BESSELING, J.F., "Non-Linear Analysis of Structures by the Finite Element Method as a Suplement to a Linear Analysis," Int. J. of Computer Methods in Appl. Mechanics and Engineering, Vol. 3, No. 2, 1974.

[5] BESSELING, J.F., "Post-buckling and Non-Linear Analysis by the Finite Element Method as a Supplement to a Linear Analysis," ZAMM 55, T3-T5, 1975.

[6] ARGYRIS, J.H., KÖNIG, M., NAGY, D.A., HAASE, M., and MALEJANNAKIS, G., "Geometric Nonlinearity and the Finite Element Displacement Method," Conference on Numerical Methods in Non-Linear Mechanics, Jablonna (Warsaw), Poland, Sept. 1974 (also contained in ISD Report 174, Stuttgart, 1975).

[7] NAGY, D.A., "Geometrically Nonlinear Finite Element Behavior Using Buckling Mode Superposition," Int. J. of Computer Methods in Applied Mechanics and Engineering (to appear).

[8] TIMOSHENKO, S., AND GERE, J., Theory of Elastic Stability, McGraw-Hill, New York, 1961.

[9] RUTISHAUSER, H., "Computational Aspects of F.L. Bauer's Simultaneous Iteration Method,"

[10] SCHREM, E., "A Short Description of the ASKA System," I.S.D. ASKA UM-215, University of Stuttgart, 1975.

[11] NAGY, D.A., "ASKA Part III-2-Linear Buckling: Lecture Notes and User's Guide," ISD Report 153 (ASKA UM 210), Stuttgart, 1974.

[12] KERR, A.D., and SOIFER, M.T., "The Linearization of the Prebuckling State and its Effect on the Determined Instability Loads," Journal of Applied Mechanics, Trans. of the ASME, 1969.

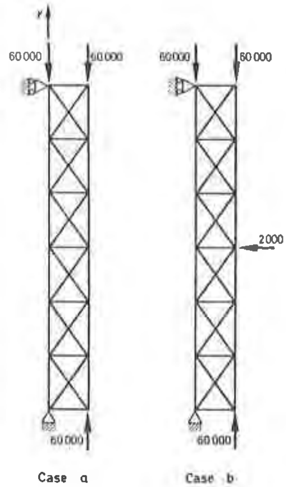

Figure 1: Braced Truss Tower and Loading Cases

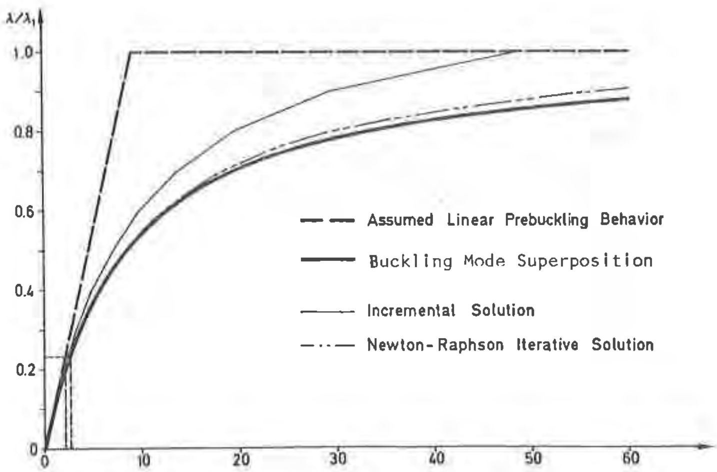

Figure 2: Lateral Displacement at Midheight vs. Applied Loading Factor (λ/λ_1)

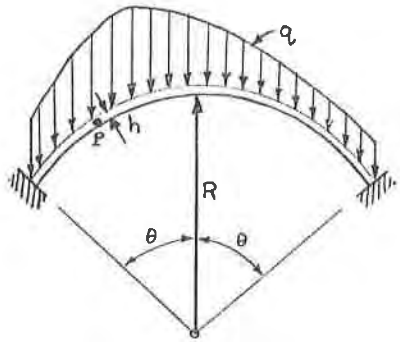

Figure 3: Circular Arch Segment Under Axisymmetric Vertical Loading

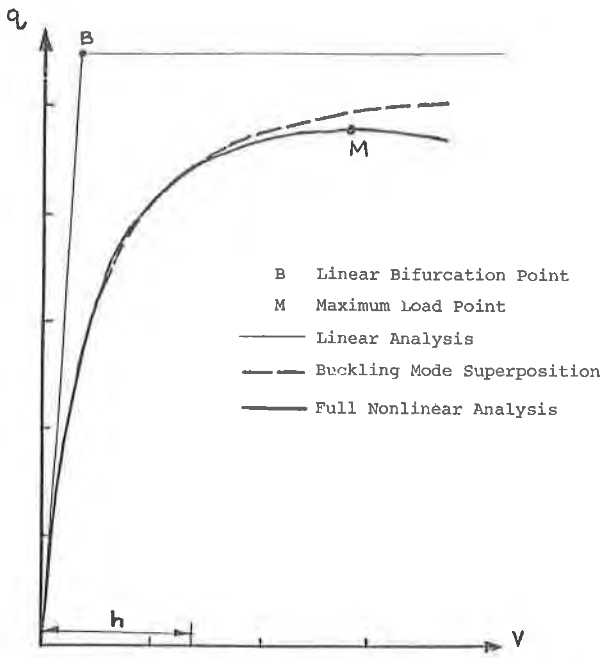

Figure 4: Radial Displacement at Point P